



저작자표시-비영리-변경금지 2.0 대한민국

이용자는 아래의 조건을 따르는 경우에 한하여 자유롭게

- 이 저작물을 복제, 배포, 전송, 전시, 공연 및 방송할 수 있습니다.

다음과 같은 조건을 따라야 합니다:



저작자표시. 귀하는 원저작자를 표시하여야 합니다.



비영리. 귀하는 이 저작물을 영리 목적으로 이용할 수 없습니다.



변경금지. 귀하는 이 저작물을 개작, 변형 또는 가공할 수 없습니다.

- 귀하는, 이 저작물의 재이용이나 배포의 경우, 이 저작물에 적용된 이용허락조건을 명확하게 나타내어야 합니다.
- 저작권자로부터 별도의 허가를 받으면 이러한 조건들은 적용되지 않습니다.

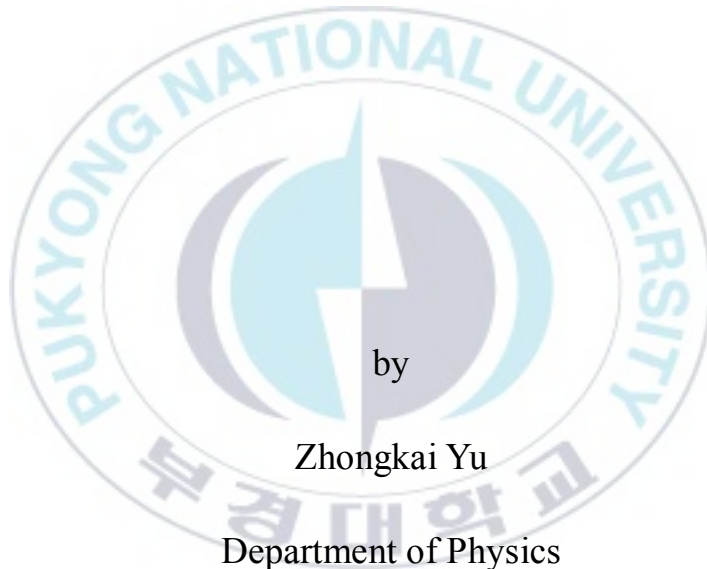
저작권법에 따른 이용자의 권리는 위의 내용에 의하여 영향을 받지 않습니다.

이것은 [이용허락규약\(Legal Code\)](#)을 이해하기 쉽게 요약한 것입니다.

[Disclaimer](#)

Thesis of Degree of Master of Natural Science

**A Study on Charge Transport Layer for
High Performance Organic and
Perovskite Light-Emitting Diodes**



by

Zhongkai Yu

Department of Physics

The Graduate School

Pukyong National University

August 2020

A Study on Charge Transport Layer for High Performance Organic and Perovskite Light-Emitting Diodes

(고성능 유기 및 페로브스카이트
발광소자를 위한 전하수송층 연구)

Advisor : Prof. Bo Ram Lee

by
Zhongkai Yu

A thesis submitted in partial fulfillment of the requirements
for the degree of

Master of Natural Science
in Department of Physics, The Graduate School,

Pukyong National University

August 2020

A Study on Charge Transport Layer for High Performance Organic
and Perovskite Light-Emitting Diodes

A dissertation

by

Zhongkai Yu

Approved by

(Chairman) **Sung Heum Park**

(Member) **Bo Ram Lee**

(Member) **Sangwook Wu**

August 2020

Contents

List of Figures	iii
List of Tables	v
Abstract.....	vi
Chapter 1. Introduction.....	1
1.1 Introduction to PEDOT:PSS.....	1
1.2 History of OLEDs.....	2
1.3 History of PeLEDs.....	2
1.4 Introduction to Perovskite Materials.....	3
1.5 Working Principle of OLEDs and PeLEDs.....	4
1.6 Characterization of PeLEDs and OLEDs.....	7
1.6.1 Turn-on and Operating Voltage.....	7
1.6.2 Device Efficiency.....	7
Chapter 2. Research Background.....	8
Chapter 3. Experiment section.....	11
3.1 Materials.....	11
3.2 Preparation of Modified PEDOT:PSS.....	12
3.3 Devices Fabrication.....	13
Chapter 4. Result and Discussion.....	15
4.1 Device Structure and Composition.....	15
4.2 Water Stability Test.....	17
4.3 Contact Angle.....	19
4.4 AFM and SEM.....	20
4.5 Performances of PeLEDs and OLEDs.....	21
4.6 Characterization of Hole-only Devices.....	26
4.7 Time-Correlated Single Photon Counting.....	27
4.8 Device Stability.....	29

Chapter 5. Conclusion31
Reference32
Acknowledgement.....43



List of Figures

Figure 1. Chemical structure of PEDOT (top) and PSS (bottom).....	1
Figure 2. Structure of perovskite materials.....	4
Figure 3. Principle of OLEDs and PeLEDs.....	6
Figure 4. Schematic band diagrams of OLEDs and PeLEDs.....	7
Figure 5. The preparation process of water resistant PEDOT:PSS HTL.....	13
Figure 6. Schematic illustrations of (a,i) PeLEDs and (a,ii) OLEDs. Chemical structure of (b,i) perovskite and (b,ii) organic materials for emissive layer. Chemical structure of (c,i) pristine PEDOT:PSS, (c,ii) PDA and (c,iii) PCDSA.....	16
Figure 7. Energy level diagrams of (a) PeLEDs and (b) OLEDs.....	17
Figure 8. Water stability test for water dropped HTLs before and after heating.....	18
Figure 9. Contact angles of water dropped on different PEDOT:PSS films.....	20
Figure 10. AFM images of diferent PEDOT:PSS films.....	21
Figure 11. SEM images of perovskite films coated on different PEDOT:PSS films.....	21
Figure 12. Device performances of (a-c) PeLEDs and (d-f) OLEDs depending on different HTLs. (a,d) J-V, (b-e) L-V and (c,f) LE-V.....	24
Figure 13. The normalized electroluminescence (EL) spectra of PeLEDs and OLEDs with different PEDOT:PSS HTLs.....	25
Figure 14. Hole-only devices structure of (a) PeLEDs and (b) OLEDs.....	27

Figure 15. Hole-only devices characteristic of (a) PeLEDs and (b) OLEDs.27

Figure 16. Time-resolved PL signal of (a) perovskite, (b) organic film with different HTLs.29

Figure 17. Device stability of (a) PeLEDs and (b) OLEDs with pristine PEDOT:PSS and modified PEDOT:PSS.....30



List of Tables

Table1. 1	Summarized device performances of PeLEDs and OLEDs depending on different HTLs	25
-----------	--	----



A Study on Charge Transport Layer for High Performance Organic and Perovskite Light-Emitting Diodes

Zhongkai Yu

Department of Physics, The Graduate School,
Pukyong National University

Abstract

Poly(3,4-ethylenedioxythiophene):poly-styrene sulfonate (PEDOT:PSS) have been most commonly used as a hole transport materials in optoelectronic devices such as organic-based and perovskite-based solar cells and light-emitting diodes because of its proper work function and conductivity. Moreover, PEDOT:PSS is suitable for the flexible device and roll-to-roll device by solution processing. However, PEDOT:PSS has hygroscopic properties, and the water molecules it attracts can damage the active layer of devices, leading to reduced device stability. Here, we modify PEDOT:PSS and provide the water-stable hole transport layer (HTL) in perovskite light-emitting diodes (PeLEDs) and organic light-emitting diodes (OLEDs) via simple and effective method, which results in the enhanced long-term stability of both devices, compared to PeLEDs and OLEDs with pristine PEDOT:PSS.

고성능 유기 및 페로브스카이트 발광소자를 위한 전하수송층 연구

Zhongkai Yu

부경대학교 대학원 물리학과

요약

Poly(3,4-ethylenedioxythiophene):poly-styrene sulfonate (PEDOT:PSS) 는 뛰어난 전기 전도도와 일함수로 인해 유기물 및 페로브스카이트 기반 태양전지와 발광다이오드 등과 같은 광전소자에서 정공 수송 물질로 널리 사용되고 있다. 특히, PEDOT:PSS 는 용액공정이 가능하여 플렉서블 소자 및 롤투롤(roll-to-roll) 공정에 적합하다. 하지만, PEDOT:PSS 는 흡습성으로 인해 활성층의 손상과 이로 인한 소자 안정성의 감소를 초래한다. 본 연구에서는 간단하고 효과적인 방법을 통해, 높은 물 안정성을 갖는 PEDOT:PSS 기반 정공 수송 층을 개발하였으며, 이를 페로브스카이트 및 유기 발광다이오드에 적용하여 기존의 PEDOT:PSS 기반의 발광다이오드에 비해 소자의 안정성을 큰 폭으로 향상시켰다.

Chapter 1. Introduction

1.1 Introduction to PEDOT:PSS

Poly(3,4-ethylenedioxythiophene):poly-styrene sulfonate (PEDOT:PSS) is a widely used hole transport material in optoelectronic devices such as organic-based and perovskite-based solar cells and light-emitting diodes. PEDOT:PSS is composed of PEDOT and PSS two parts, PEDOT is a conductive polymer that is difficult to dissolve in water, therefore, the researchers introduced PSS part, which is easily soluble in water, developed stable PEDOT:PSS aqueous solution. The chemical structure of PEDOT (top) and PSS (bottom) is shown in Figure 1. PEDOT: PSS can be spin-coated into a uniform film on substrate with high transmittance and conductivity, and PEDOT: PSS film has excellent thermal stability, there is no obvious change in conductivity after heating at 100°C for 1000 h. [1] The work function of PEDOT: PSS (~ 5.1 eV) is well matched with the material of active layer and PEDOT:PSS is suitable for the flexible device and roll-to-roll device by solution processing.

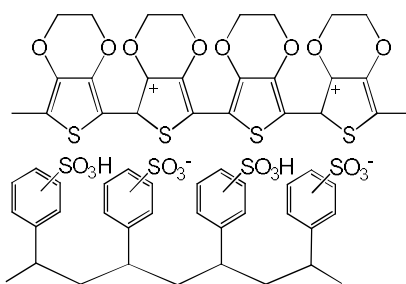


Figure 1. Chemical structure of PEDOT (top) and PSS (bottom).

1.2 History of OLEDs

In 1963, Martin Pope et al. first reported organic light-emitting diodes with anthracene single crystals. [2] In 1987, C.W. Tang from Kodak first reported a classic three layers device structure with a hole transport layer, [3] an electron transport layer and small molecules active interlayer, this classic sandwich device structure effectively controls the injection and extraction of carriers, its the basis for the development of organic light emitting diode devices. Subsequently, R.H. Friend et al. from University Cambridge made the first polymer light-emitting diodes (PLEDs) with p-phenylene vinylene (PPV) in 1990. [4] After two years, A.J. Heeger et al. Prepared flexible PLED devices for the first time, [5] showed the application prospects of organic light emitting devices.

1.3 History of PeLEDs

In 2014, R. H. Friend's group reported organic-inorganic hybrid perovskite light-emitting diodes at room temperature by solution spinning process for the first time [6], they got the emission from near infrared to green by adjusting the composition and proportion of halogen, this work opened the door to PeLEDs research. The next year, Tae-Woo Lee's research team produced a MAPbBr₃ perovskite device with a current efficiency of 42.9 cd/A [7], they created the nanocrystal pinning (NCP) spin coating process that reduced the perovskite grain

size, improved the morphology of perovskite film, and reduced the exciton quenching due to lead atoms by accurately adding methylammonium bromide (MABr). The result was published in Science and caused widespread concern in the academic community. In late 2018, Zhanhua Wei's team reported a quasi-core/shell structure device with MABr shell passivated Cs-based perovskite and achieved an external quantum efficiency (EQE) of 20.3%, [8] they created a new record for green PeLED. At present, the EQE of green [8] and red [9] PeLEDs have exceeded 20%, the efficiency of near-infrared device has reached 21.6% [10], and blue PeLEDs have also achieved EQE of 11% [11].

1.4 Introduction to Perovskite Materials

Perovskite materials are a class of compounds with the same crystal structure with calcium titanate (CaTiO_3), the structural formula of perovskite materials is generally written as “ ABX_3 ”, “A” site is monovalent cation such as methylammonium (MA^+), formamidinium (FA^+) and Cs^+ , “B” site is divalent metal cation such as Pb^{2+} and Sn^{2+} , “X” site is halide anion such as I^- , Br^- and Cl^- . In the perovskite material crystal structure of ABX_3 , “A” monovalent cations occupy eight apex angles, “B” divalent metal cations are located at the body center, and “X” halide anions occupy six face centers. As shown in Figure 2, “B” cations coordinate with six “X” anions to form an octahedra, octahedras are

connected by vertices to form three-dimensional perovskite, one “A” cation in the middle of four octahedras. We judge the stability of cubic perovskite structure by octahedron factor μ [12] and Goldschmidt’s tolerance factor t [13], the calculation formulas are $(R_A + R_X) = t\sqrt{2}(R_B + R_X)$ and $\mu = R_B/R_X$, here, R_A , R_B and R_X respectively represent the ionic radius of “A”, “B”, and “X” ions. When $0.80 < t < 1.03$, $\mu > 0.442$, [14] stable cubic perovskite structure can be formed.

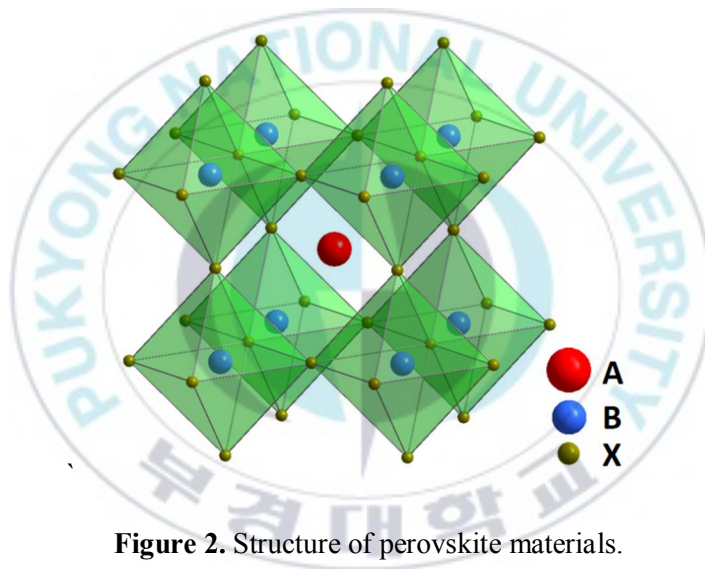


Figure 2. Structure of perovskite materials.

1.5 Working Principle of OLEDs and PeLEDs

Electroluminescence is a phenomenon in which a luminescent material converts electrical energy into light energy under the applied electric field. When a voltage is applied to the electrodes of OLEDs and PeLEDs, holes and electrons

are injected from the anode and cathode, respectively. After the holes and electrons are transported to emissive layer, they will recombine to form electron-hole pairs, which are excitons. Finally, excitons will return to the ground state by radiative transition to realize light emission. This process can be divided into the following three steps: (1) Charge injection and transport, (2) Exciton formation, (3) Exciton radiative transition

Under the applied voltage, holes are injected from the anode to the highest occupied molecular orbital (HOMO) of the light-emitting layer, electrons are injected into the lowest unoccupied molecular orbital (LUMO) of the emissive layer at the cathode. The injection barrier comes from the difference between the work function of the device electrode material and the HOMO and LUMO levels of the emissive layer. Therefore, we usually use metal with low work function as the cathode and ITO with higher work function as the anode, and treat the ITO with ultraviolet ozone or plasma to improve the work function of the anode. After the charge carriers are injected, they move and drift in two directions under the applied electric field. Carrier mobility can be measured by space-charge limited current (SCLC).

Due to coulomb forces, electron and hole will recombine into hole-electron pair (exciton), typically, the mobility of holes in device is higher than electrons, excitons will form near the cathode and quench. Therefore, introducing suitable HTL and ETL can be used to control carriers migration and achieve balanced

charge transport. The excitons decay from the excited state to the ground state by radiative transitions, and at the same time release photons, so the device emits light. Theoretically, the generated excitons are singlet excitons and triplet excitons in a ratio of 1: 3. Fluorescent materials can only release photons using singlet excitons radiation transition, Phosphorescent material-based light-emitting devices can use all excitons during the light emission process, the theoretical internal quantum efficiency can reach 100%, which is 4 times that of fluorescent material-based light-emitting devices.

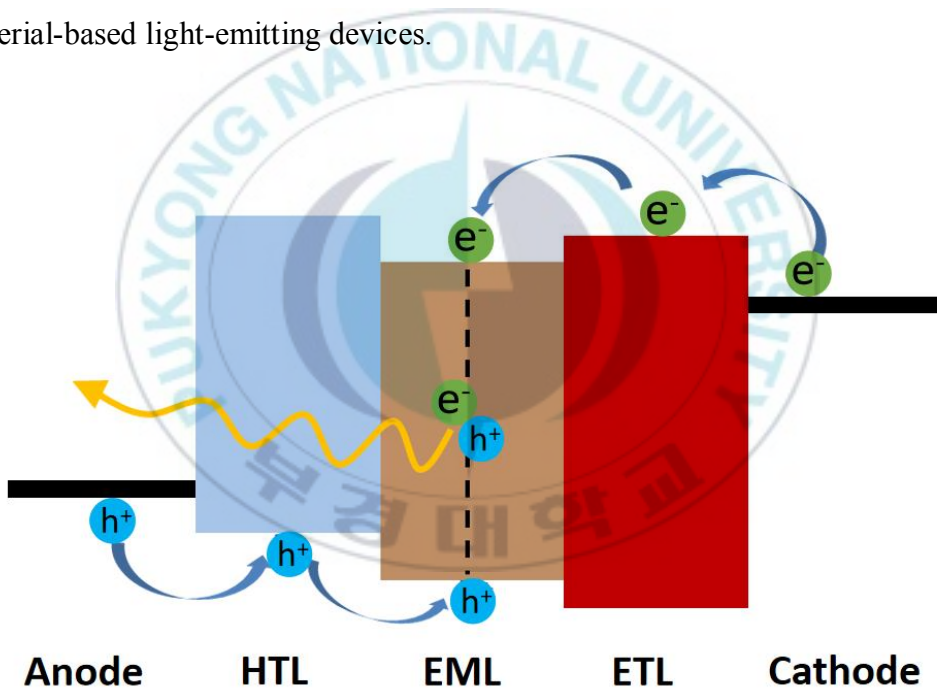


Figure 3. Principle of OLEDs and PeLEDs

1.6 Characterization of PeLEDs and OLEDs.

1.6.1 Turn-on and Operating Voltage

As shown in Figure 4, if device at zero bias condition, the tunneling is not able to take place due to the tilt of energy band. When the applied voltage equals to the difference of the work functions of the anode and cathode, “flat band” condition occurs, the turn-on voltage is the minimum voltage for electrons and holes injection. When the current starts to quickly increase, it means holes and electrons can be injected into the active layer by tunneling, we call this voltage the operating voltage. [15]

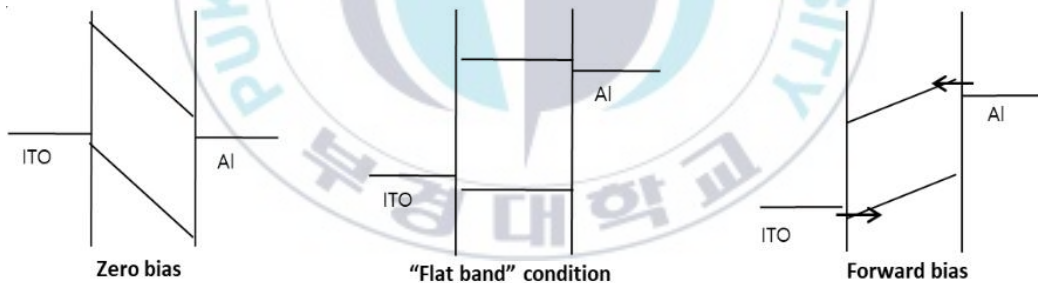


Figure 4. Schematic band diagrams of OLEDs and PeLEDs.

1.6.2 Device Efficiency

We generally use current efficiency and external quantum efficiency to characterize the luminous efficiency of LED. The current efficiency (CE) of

device is defined as the luminous brightness at unit current density, the unit is cd/A, the calculation formula is as follows:

$$\text{Current Efficiency(cd/A)} = \frac{\text{luminance}}{\text{current density}}$$

The external quantum efficiency (EQE) of device is the ratio of the number of photons emitted to the outside of the device to the number of electrons injected into the external circuit, as shown in the following formula:

$$\text{EQE} = \frac{\text{the number of emitted photons}}{\text{the number of injected electrons}}$$

Chapter 2. Research Background

Recently, organic- and perovskite-based light-emitting diodes (OLEDs and PeLEDs) have been investigated extensively for display, solid-state lighting and flexible electronic devices because of their attractive advantages such as low cost, easy fabrication and flexible mechanical properties.[4, 6, 8-9, 16-21] OLEDs have gradually moved from the laboratory to the factory due to their advantages of self-illumination, quick response, ultra-thin and flexibility. From 2014, R. H. Friend's team first reported organic-inorganic hybrid perovskite light-emitting

diodes at room temperature to the present, the efficiency of green light devices is getting closer to the theoretical value, the efficiency of red and blue light devices is also increasing year by year. Extensive efforts have been dedicated to enhance the device efficiency via the device optimization including interfacial engineering/surface modification [22-26] and synthesis of emissive materials with a high quantum yield[27-31]. Basically, p-i-n conventional structure consists of indium tin oxide (ITO) as a transparent anode, poly(3,4-ethylenedioxythiophene):poly-styrene sulfonate (PEDOT:PSS) as a hole transport layer (HTL), an emissive layer, lithium fluoride (LiF) as an electron injection/transporting layer (EIL/ETL) and aluminum (Al) as a metallic cathode. PEDOT:PSS and LiF can reduce the contact barrier between anode/emissive layer and cathode/emissive layer, respectively, which cause well-balanced charge injection/transport, leading to high device efficiency.[8-9, 23, 32] However, PEDOT:PSS has a few critical disadvantages in organic- and perovskite-based optoelectronic devices despite the fact that PEDOT:PSS is an efficient HTL. The strong acidic (pH ~1) and hygroscopic properties of PEDOT:PSS can gradually corrode an ITO electrode[33-35] and can damage in the active layer from water molecules[36-37], which results in eventually degradation of the device performance and long-term stability. Moreover, significant quenching of radiative excitons normally occurs at the interface between PEDOT:PSS and an emissive layer due to high electric conductivity.[38-40] Thus, there is still considerable

room for further enhancements in performance and stability of PeLEDs and OLEDs via improved HTLs.

Extensive efforts have been dedicated to develop efficient HTLs alternatives to PEDOT:PSS for the improvement of device performance and long-term stability. Basically, p-type metal oxide thin films such as nickel oxide (NiO_x) [41-42], tungsten oxide (WO_3) [43-44] and molybdenum trioxide (MoO_x) [45-46] were reported as an effective HTL with excellent long-term stability. However, high crystalline metal oxide-based HTLs require high-temperature annealing over 400 °C [47-48] or vacuum evaporation technique [49-50]. In addition, low-temperature and solution-processable approaches by using conjugated polyelectrolytes (CPEs) [51-53] and graphene oxide (GO) [54-56] were introduced for an efficient HTL in PeLEDs and OLEDs.

Coated emissive layer on top of CPEs can induce the non-uniform morphology depending on the surface property of CPEs. [53] In particular, an emissive layer using perovskite materials is more sensitive than those using organic materials. GO-based HTLs is difficult to obtain the full-coverage films via a time. [54] Furthermore, this method is not easily to control the thickness of HTL. The device performances were significantly changed depending on the thickness of GO.

Here, we present a simple and effective HTL by introducing modified PEDOT:PSS with 2-pentacosyl-10,12-diamidoethylsulfate (PCDSA) as a photo-

crosslinking agent in both PeLEDs and OLEDs. PCDSA converted to polydiacetylenes (PDAs) after UV irradiation, which results in water-resistant property. [57-58] Water-stable PEDOT:PSS prevents the penetration of water into the emissive layer of OLEDs and PeLEDs, which results in the enhanced device stability. Moreover, modified HTL can decrease the quenching of radiative excitons at the interface between HTL and an emissive layer due to the reduction of conductivity of PEDOT:PSS. In particular, optimized devices with modified HTL show maximum luminance of 3,600 cd m⁻² and luminous efficiency (*LE*) of 15.2 cd A⁻¹ in PeLEDs and maximum luminance of 33,700 cd m⁻² and *LE* of 12.9 cd A⁻¹ in OLEDs, which are comparable to both reference devices using pristine PEDOT:PSS.

Chapter 3. Experiment section

3.1 Materials

ITO transparent conductive electrode (~4.5 Ω/sq, AMG) was used for anode. PEDOT:PSS aqueous solution (Clevios AI 4083) was purchased from Heraeus Clevios for HTL. 10, 12-pentacosadiynoic acid (PCDA) (GFS Chemicals) and 2-aminoethylsulfate (Sigma-Aldrich) were purchased. The perovskite precursors, lead bromide (PbBr₂) (99.999%, Alfa Aesar), benzylamine hydrobromide (BABr) (98%, Tokyo Chemical Industry) and

cesium bromide (CsBr) (99.999%, Sigma-Aldrich) were used for an emissive layer of PeLEDs.

Super yellow (SY) ($M_w = 1,950,000 \text{ g mol}^{-1}$, Merck) for an emissive material of OLEDs, 2,2',2''-(1,3,5-benzinetriyl)tris(1-phenyl-1-H-benzimidazole) (TPBi) (99.9%, OSM) as an exciton blocking layer and ETL, LiF (iTASCO 99.9%) as EIL and Al (iTASCO 99.9%) as cathode were obtained.

MoO₃ (iTASCO 99.995%) and gold (Au) (iTASCO 99.99%) were used in hole-only devices.

All solvents, namely, dimethyl sulfoxide (DMSO) (99.9%, Sigma-Aldrich), chlorobenzene (CB) (99.8%, Sigma-Aldrich) and methanol (MeOH) (99.9%, Alfa Aesar) were purchased.

3.2 Preparation of Modified PEDOT:PSS

The detailed synthesis of PCDSA materials is described in reference [57]. To prepare the water-stable HTL, PEDOT:PSS (AI 4083) was mixed with PCDSA of 5 wt.%, and then stirring at 300 °C for 3 min. Moreover, modified PEDOT:PSS solution was filtered using cellulose acetate (CA) filter to remove hot reaction residues. Filtered solution was spin-cast on an ITO-coated glass substrate. The modified PEDOT:PSS film containing PCDSA was treated by UVO for 3 min, and then annealed at 140 °C for 10 min for the fabrication of the photo-crosslinked film surface.

3.3 Devices Fabrication

ITO was washed by ultrasonic treatment in deionized water (DI water), acetone and ethanol for 10 min respectively. After drying in oven, ITO substrate was treated with O₂ plasma for 10 min. Dissolving PCDSA in PEDOT:PSS (AI 4083) solution was spun on ITO at 5,000 rpm for 40 s. After UV treatment for 3min, samples were transferred to a 145 °C hot plate for annealing for 10 min. Finally, MeOH was spin coated onto the photo-crosslinked PEDOT:PSS at 3,000 rpm for 45 s, and annealed at 100 °C for 5min.

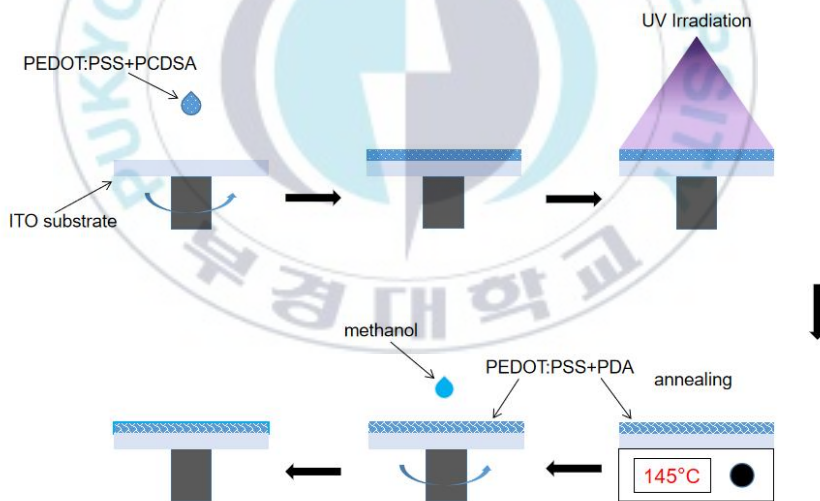


Figure 5. The preparation process of water resistant PEDOT:PSS HTL.

Quasi-2D perovskite precursor solution of 0.2M (PbBr₂, CsBr and BAbR at a molar ratio of 1:0.67:0.67) was dissolved in DMSO at 60 °C. To form an emissive layer of PeLEDs, the perovskite precursor solution was spin coated on HTL at 5,000 rpm for 40 s; after 5 s of spin-coating at 500 rpm. After 15 s of spin-coating at 5000 rpm, ~300 μL of CB was quickly dropped onto the center of the spinning substrate in a glovebox, and then annealed at 120 °C for 10 min. To form an emissive layer of OLEDs, SY solution (dissolving 6.5 mg mL⁻¹ in CB) was deposited on HTL by spin-coating at 2,000 rpm for 45 s.

Finally, TPBi (55 nm, for only PeLEDs), LiF (1 nm) and Al (100 nm) were sequentially deposited at ~ 10⁻⁶ Torr by the thermal evaporation method.

Hole-only devices were fabricated similarly with PeLEDs and OLEDs, except parts of LiF and Al. For hole-only devices, MoO₃ (10 nm) and Au (100 nm) were used by the thermal evaporation method instead of LiF and Al.

Chapter 4. Result and Discussion

4.1 Device Structure and Composition

Figure 6ab shows the device architectures of (a,i) PeLEDs and (a,ii) OLEDs and the chemical structure of emissive layers; (b,i) quasi-2D perovskite $\text{BA}_2\text{Cs}_2\text{Pb}_3\text{Br}_{10}$ ($n=3$) of PeLEDs and (b,ii) super yellow (SY) of OLEDs. Both devices has p-i-n structure, which were composed of transparent ITO as anode, modified PEDOT:PSS as HTL, LiF as ETL/EIL and Al as cathode with emissive layers of PeLEDs and OLEDs, respectively. In PeLEDs, TPBi was additionally used as ETL and exciton blocking layer. The diagrams of PeLEDs and OLEDs for flat band conditions are shown in Figure 7. Figure 6c presents the chemical structure of elements such as (i) PEDOT:PSS, (ii) PCDSA and (iii) polydiacetylenes (PDAs).

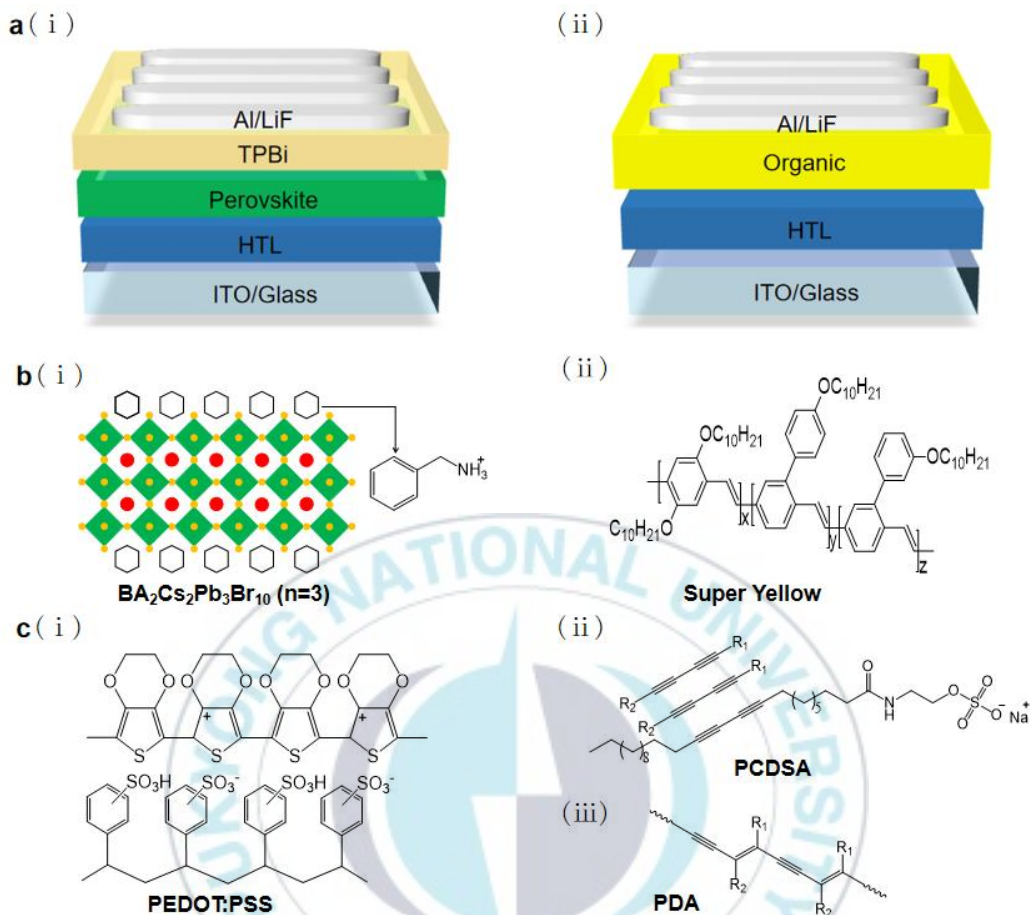


Figure 6. Schematic illustrations of (a,i) PeLEDs and (a,ii) OLEDs. Chemical structure of (b.i) perovskite and (b.ii) organic materials for emissive layer. Chemical structure of (c.i) pristine PEDOT:PSS, (c.ii) PDA and (c.iii) PCDSA.

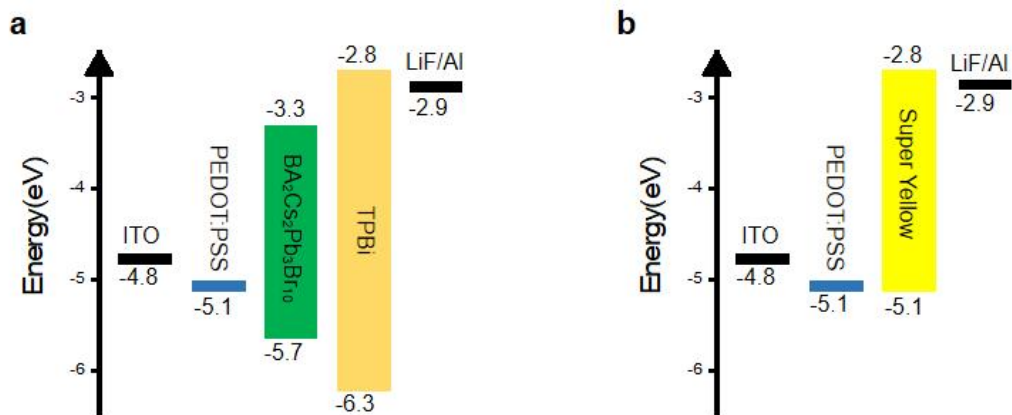


Figure 7. Energy level diagrams of (a) PeLEDs and (b) OLEDs.

4.2 Water Stability Test

UV irradiation can induce the photo-polymerization of PCDSA molecules, which results in the formation of PDAs inside the PEDOT:PSS film, leading to water-stable HTL.[58] We conducted a water stability test for the PEDOT:PSS+PDA film, PEDOT:PSS+PDA(MeOH) film and pristine PEDOT:PSS film. After prepared samples, DI water dripped on the prepared samples. Heating process was applied to pristine PEDOT:PSS film and modified PEDOT:PSS films at 150 °C for water evaporation on surface. As shown in Figure 8a-f, pristine PEDOT:PSS film was obviously created droplet-shaped edges. In contrast, there was no obvious damage on the surface of PEDOT:PSS+PDA film and PEDOT:PSS+PDA(MeOH) film. These results show the successful modification of the PDA in PEDOT:PSS

film by UV-irradiation. In other words, this indicates that the PDA modification in PEDOT:PSS strengthens the water resistance.

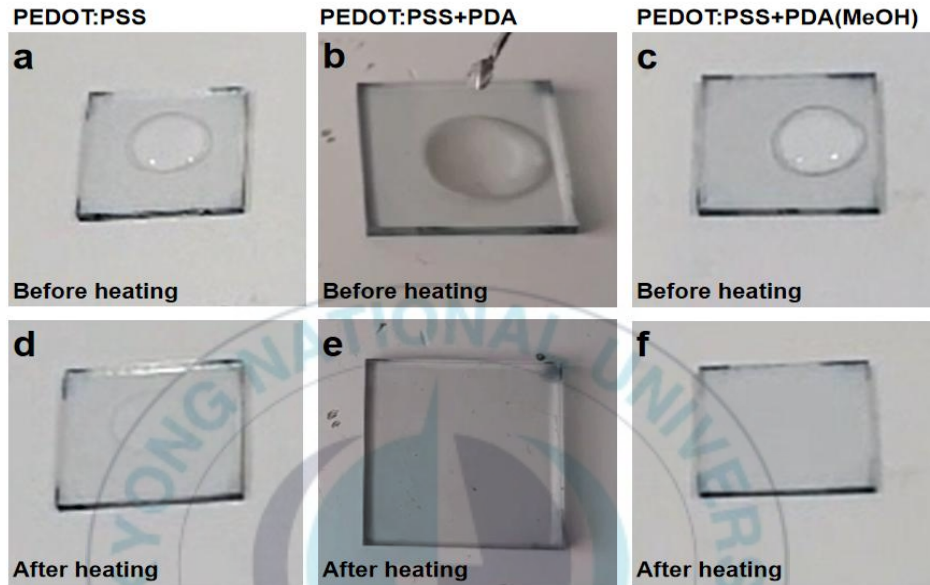


Figure 8. Water stability test for water dropped HTLs before and after heating.

However, the electrical conductivity of water-stable PEDOT:PSS film was reduced due to PDA as an insulator, leading to inefficient hole injection and transport whereas modified HTL has water-stable property. Thus, MeOH was used for recovering reduced conductivity of modified PEDOT:PSS by removing insulating PSS parts and PDA residues.[59]

4.3 Contact Angle

To check the hydrophilicity of PEDOT:PSS films with different treatment, we measured contact angles by SmartDrop instrument (FemtoBiomed incorporated). Figure 9 shows the measurement of contact angle depending on the different HTLs; (a) pristine PEDOT:PSS, (b) PEDOT:PSS+PDA and (c) PEDOT:PSS+PDA with MeOH treatment. The contact angle of a pristine PEDOT:PSS film was observed to be 6 °. After UV irradiation for cross-linking process, the contact angle increased to 15.4°. This indicates that the hydrophilicity of the PDA-produced film was reduced compared to the PEDOT:PSS film. Previous studies have shown that PDAs are much more hydrophobic than in the monomer (PCDSA) state. [57] The change in contact angle is result of PDAs formation in the PEDOT:PSS matrix. And after MeOH treatment, the contact angle increased slightly to 20.7°. The reason for this phenomenon is that when the film is treated with a polar solvent such as methanol, a small amount of PSS can be removed, which increases the PEDOT ratio in PEDOT:PSS film.[60]



Figure 9. Contact angles of water dropped on different PEDOT:PSS films.

4.4 AFM and SEM

In order to study the effect of the addition of photo-crosslinking agent and methanol treatment on the morphology of PEDOT:PSS film, atomic force microscopy (AFM) images of various PEDOT:PSS films are presented, as shown in Figure 10. The morphologies and the roughness values of the three sample surfaces are similar (rms roughness= 0.92, 1.06, and 1.01 nm respectively). These AFM results confirm that various HTLs were well-coated and PDAs and MeOH treatment do not affect the morphology of PEDOT:PSS.

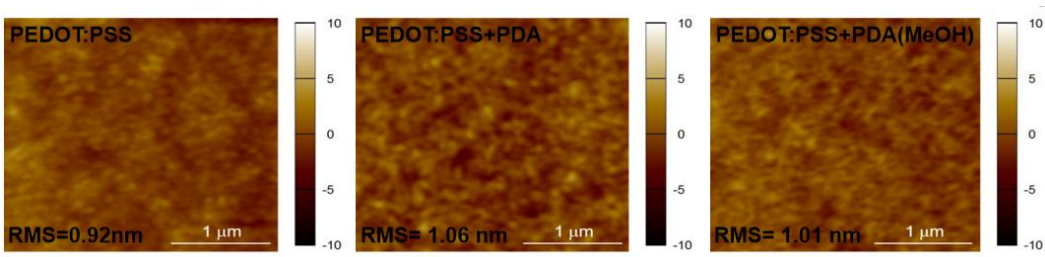


Figure 10. AFM images of different PEDOT:PSS films.

To investigate the crystallinity of the perovskite film on various HTLs, the scanning electron microscopy (SEM) image was performed as shown in Figure 11. As we observed, all the perovskite films were well-coated and well-grown on the different HTLs



Figure 11. SEM images of perovskite films coated on different PEDOT:PSS films.

4.5 Performances of PeLEDs and OLEDs.

The current density-voltage-luminance (J - V - L) and LE of the PeLEDs and OLEDs were measured using a computer-controlled Keithley 2450 Source Meter and a TOPCON spectroradiometer (SR-3AR, TOPCON)

under ambient conditions. Figure 12 presents the device characterizations including current density versus voltage (J - V), luminance versus applied voltage (L - V) and luminous efficiency versus voltage (LE - V) of optimized (a-c) PeLEDs and (d-f) OLEDs with various HTLs such as PEDOT:PSS, PEDOT:PSS+PDA and PEDOT:PSS+PDA with MeOH treatment.

The optimized PeLEDs with PEDOT:PSS (reference device) exhibited a maximum luminance of $4,400\text{cd m}^{-2}$ and maximum LE of 15.4 cd A^{-1} . However, optimized PeLEDs with PEDOT:PSS+PDA, which are a maximum luminance of $2,600\text{cd m}^{-2}$ and maximum LE of 7.0 cd A^{-1} , decreased the device performances, compared to the reference device. The reason why the device performance decreased is the inefficient injection and transport of holes from ITO anode to perovskite emissive layer, which results from reduced electrical conductivity of PEDOT:PSS by PDAs.

On the other hand, the device performances of optimized PeLEDs using PEDOT:PSS+PDA with MeOH treatment are similar to those of reference devices. This device exhibited a maximum luminance of $3,600\text{cd m}^{-2}$ and maximum LE of 15.2 cd A^{-1} . MeOH treatment can increase the electrical conductivity of PEDOT:PSS by removing the small amount of PSS and PDAs residues, leading to the improved hole injection and transport.

Moreover, the phenomenon of device characterizations in PeLEDs is shown similarly in OLEDs. The device performances of optimized OLEDs

with PEDOT:PSS (reference device) were a maximum luminance of 41,200cd m⁻² and maximum *LE* of 13.1 cd A⁻¹, whereas those of OLEDs with PEDOT:PSS+PDA were a maximum luminance of 19,900cd m⁻² and maximum *LE* of 11.3 cd A⁻¹. These values were slightly reduced, compared to those of reference device. However, the device performances of OLEDs with PEDOT:PSS+PDA were recovered after MeOH treatment, which are comparable to the reference device.

Depending on different HTLs, the difference of devices performances in OLEDs were less than those in PeLEDs. We consider results from relatively effective hole injection and transport in comparison with PeLEDs. In general, the energy barrier between SY of ~ 5.1 eV and PEDOT:PSS of ~5.1 eV almost never in OLEDs, leading to ohmic contact. Thus, hole transport can be dominantly determined by the difference of electrical conductivity according to HTLs. On the other hand, larger energy barrier of ~ 0.6 eV between perovskite emissive layer of ~5.7 eV and PEDOT:PSS of ~5.1 eV exist in PeLEDs. Low electrical conductivity is more difficult to inject and transport holes at the interface between perovskite emissive layer and PEDOT:PSS+PDA due to large energy barrier, compared to reference device with PEDOT:PSS. However, the electrical conductivity of PEDOT:PSS+PDA after MeOH treatment increase again, which results in the effectively hole injection and transport at the interface

between HTL and an emissive layer, leading to the enhanced devices performances.

Detailed device characteristics with various HTLs are summarized in Table 1, and EL spectra of PeLEDs and OLEDs with different HTLs are shown in Figure 13, The EL spectra of PeLEDs exhibit very narrow peaks with a full width at half maximum (FWHM) of 22 nm and there is no obvious shift in all EL peaks.

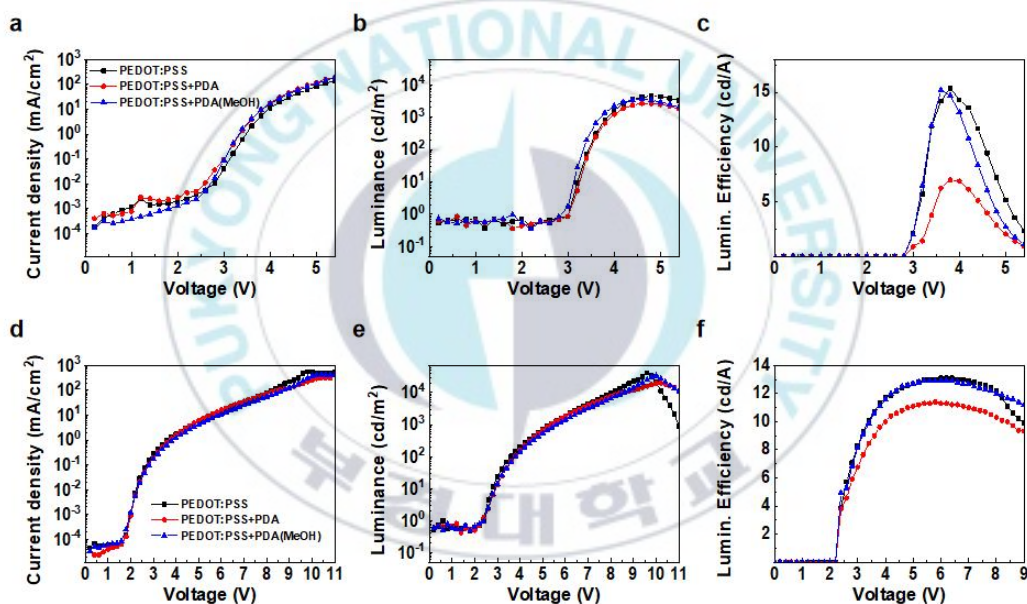


Figure 12. Device performances of (a-c) PeLEDs and (d-f) OLEDs depending on different HTLs. (a,d) J - V , (b-e) L - V and (c,f) LE - V .

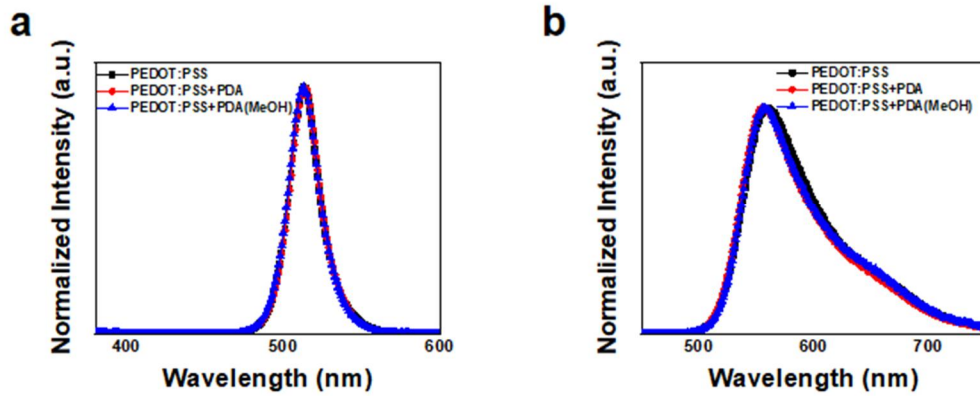


Figure 13. The normalized electroluminescence (EL) spectra of PeLEDs and OLEDs with different PEDOT:PSS HTLs.

Table 1. Summarized device performances of PeLEDs and OLEDs depending on different HTLs.

Device Configuration	L_{\max} [cd/m^2] (@ bias [V])	CE_{\max} [cd/A] (@ bias [V])	Turn-on voltage [V] (@ 1 cd/m^2)
ITO / PEDOT:PSS / $\text{BA}_2\text{Cs}_2\text{Pb}_3\text{Br}_{10}$ / TPBi / LiF / Al	4400@4.8	15.4@3.8	3.0
ITO / PEDOT:PSS+PDA / $\text{BA}_2\text{Cs}_2\text{Pb}_3\text{Br}_{10}$ / TPBi / LiF / Al	2600@4.6	7.0@3.8	3.0
ITO / PEDOT:PSS+PDA(MeOH) / $\text{BA}_2\text{Cs}_2\text{Pb}_3\text{Br}_{10}$ / TPBi / LiF / Al	3600@4.6	15.2@3.6	3.0
ITO / PEDOT:PSS / Super Yellow / LiF / Al	41200@9.6	13.1@6.0	2.4
ITO / PEDOT:PSS+PDA / Super Yellow / LiF / Al	19900@10.2	11.3@5.4	2.4
ITO / PEDOT:PSS+PDA(MeOH) / Super Yellow / LiF / Al	33700@10.0	12.9@5.4	2.4

4.6 Characterization of Hole-only Devices

To more investigate the injection and the transport of holes at the interface between different HTLs and emissive layers in PeLEDs and OLEDs, we have fabricated the hole-only devices and analyzed the J - V characteristics. The current of hole-only devices were measured under applied bias by Keithley 2400 Source Meter. Figure 14 shows the hole-only devices structure of (a) PeLEDs and (b) OLEDs. Hole-only devices used MoO_3 and Au instead of LiF and Al. More detailed preparation procedures are shown in the experimental part. The current densities were significantly different in perovskite hole-only device whereas those were slightly changed in organic hole-only device according to different HTLs, as shown in Figure 15a,b. In particular, the current density of perovskite hole-only device with PEDOT:PSS+PDA quite decreased, compare to the those with PEDOT:PSS (reference device). Moreover, the current density of perovskite hole-only device with PEDOT:PSS+PDA after MeOH treatment shows slightly reduced current density. These results strongly provide the correlation between the devices performances and hole injection/transport according to the electrical conductivity.

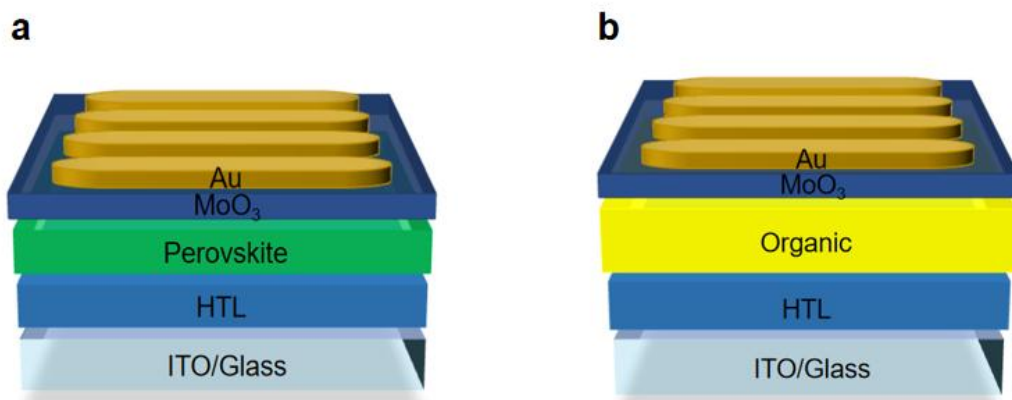


Figure 14. Hole-only devices structure of (a) PeLEDs and (b) OLEDs.

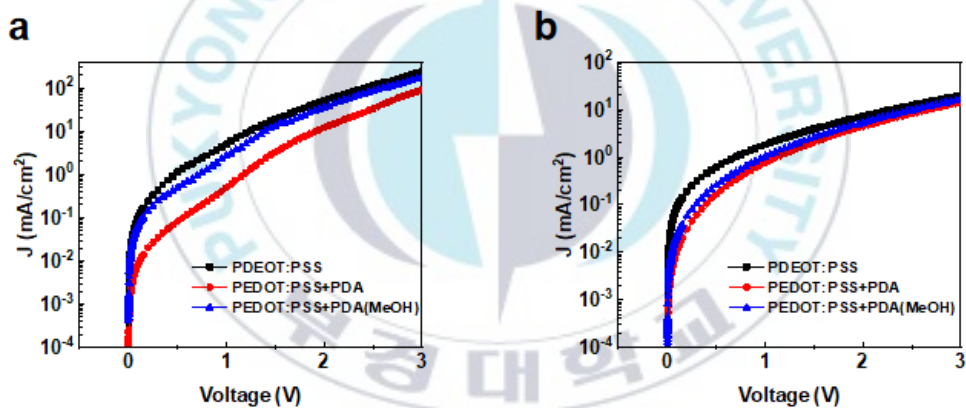


Figure 15. Hole-only devices characteristic of (a) PeLEDs and (b) OLEDs.

4.7 Time-Correlated Single Photon Counting

The photoluminescence (PL) decay depending on various HTLs were measured using time-correlated single photon counting (TCSPC) for analysis of the quenching of radiative excitons at the interface between HTLs and emissive layers, as shown in Figure 16a,b.

The initial fast decay was significantly decreased in perovskite emissive layer/PEDOT:PSS due to effective hole transport from the perovskite layer to PEDOT:PSS by excellent electrical conductivity of PEDOT:PSS. On the other hand, the fraction of initial fast decay was decreased in perovskite emissive layer/PEDOT:PSS+PDA, compared to those of perovskite emissive layer/PEDOT:PSS, indicating reduced hole transport. The film of perovskite/PEDOT:PSS+PDA with MeOH treatment show the moderate quenching rate between PEDOT:PSS and PEDOT:PSS+PDA.

On the other hand, the fraction of PL decay is almost similar in organic emissive layer/HTLs owing to ohmic contact between organic emissive layer and HTLs, but which depending on HTLs is slightly decreased by reduced electrical conductivity.

The increased PL lifetime of PEDOT:PSS+PDA can be a factor for the improvement of device efficiency, but with a trade-off in the reduced electrical conductivity that may provide inefficient hole transport. The combined results of hole-only devices characteristics and TCSPC support the correlation of device performances depending on different HTLs.

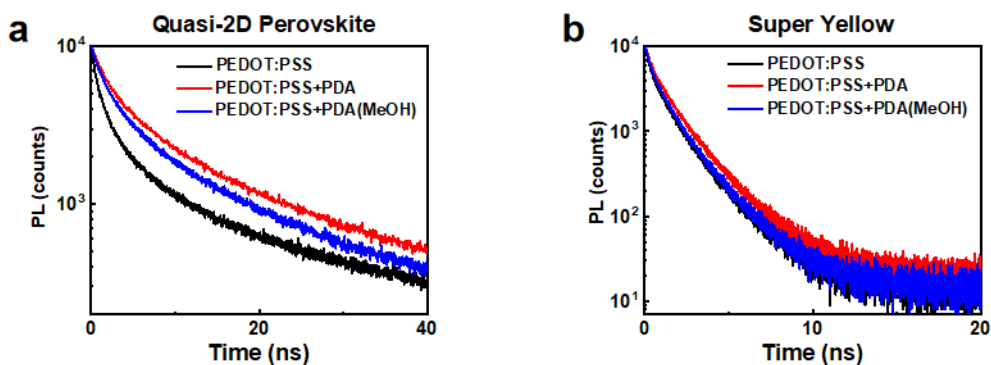


Figure 16. Time-resolved PL signal of (a) perovskite, (b) organic film with different HTLs.

4.8 Device Stability

To investigate the operational stability of devices fabricated with pristine PEDOT:PSS and modified PEDOT:PSS, the long-term stability of both PeLEDs and OLEDs were measured under ambient air conditions at an initial luminance of $\sim 100 \text{ cd m}^{-2}$ (@3.5 V in PeLEDs and @3.7 V in OLEDs). As shown in Figure 17, the luminance decay rate of the PeLED device based on pristine PEDOT:PSS is obviously higher than the device based on PEDOT:PSS with PDA and MeOH, the reference perovskite device decayed to 50% of the initial luminance in 6 min, the PeLED device based on modified PEDOT:PSS retained up to 50% of its initial luminance until 10 min, it is equivalent to increasing the half-lifetime of the PeLED device by 67%. OLEDs with modified PEDOT:PSS also present the

enhanced device stability, compared to that with pristine PEDOT:PSS. In particular, the difference of device stability in PeLEDs reacting more sensitively to moisture was more pronounced depending on HTLs.

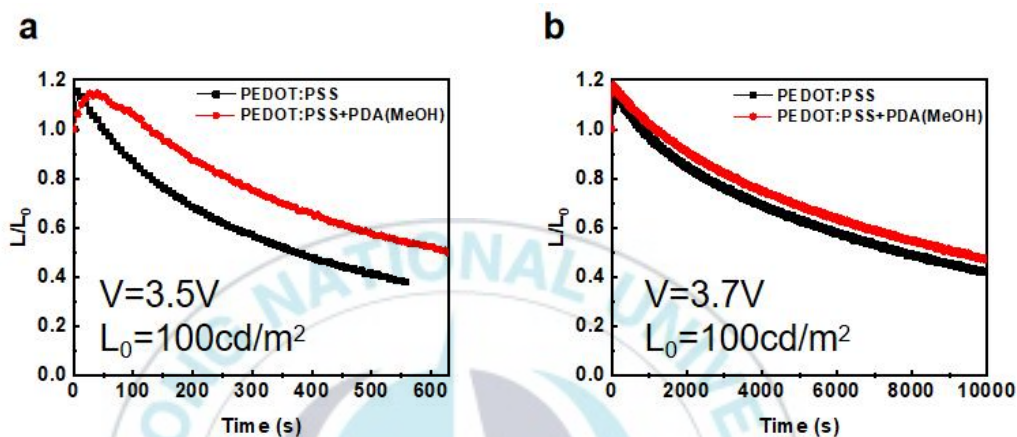


Figure 17. Device stability of (a) PeLEDs and (b) OLEDs with pristine PEDOT:PSS and modified PEDOT:PSS.

Chapter 5. Conclusion

In summary, we successfully demonstrate modified PEDOT:PSS with PDA and MeOH treatment as an water-stable HTL in both PeLEDs and OLEDs. Water-stable HTL provides simple processing and efficient hole injection/transport, which results in the improvement of device stability and comparable device performances, compared to both devices with pristine PEDOT:PSS. In particular, modified HTL is strongly stable in a moisture, which is effective in PeLEDs reacting more sensitively in moisture. Moreover, organic materials and perovskite materials for an emissive layer are well-coated on the water-stable HTL due to excellent wettability and compatibility, leading to uniform and clean film. Furthermore, we measure the hole-only devices and TCSPC to understand the correlation between the charge transport and the quenching of radiation excitons depending on various HTLs with different electrical conductivity.

Reference

- (1) Sarac, A. S. Nanofibers of Conjugated Polymers, Jenny Stanford Publishing: 2017.
- (2) Pope, M.; Kallmann, H. P.; Magnante, P. Electroluminescence in Organic Crystals. *The Journal of Chemical Physics* 1963, 38 (8), 2042-2043.
- (3) Tang, C. W.; VanSlyke, S. A. Organic electroluminescent diodes. *Applied Physics Letters* 1987, 51 (12), 913-915.
- (4) Burroughes, J. H.; Bradley, D. D. C.; Brown, A. R.; Marks, R. N.; Mackay, K.; Friend, R. H.; Burns, P. L.; Holmes, A. B. Light-Emitting Diodes Based on Conjugated Polymers. *Nature* 1990, 347, 539.
- (5) Gustafsson, G.; Cao, Y.; Treacy, G. M.; Klavetter, F.; Colaneri, N.; Heeger, A. J. Flexible light-emitting diodes made from soluble conducting polymers. *Nature* 1992, 357 (6378), 477-479.
- (6) Tan, Z. K.; Moghaddam, R. S.; Lai, M. L.; Docampo, P.; Higler, R.; Deschler, F.; Price, M.; Sadhanala, A.; Pazos, L. M.; Credgington, D.; Hanusch, F.; Bein, T.; Snaith, H. J.; Friend, R. H. Bright Light-Emitting Diodes Based on Organometal Halide Perovskite. *Nat. Nanotechnol.* 2014, 9, 687.
- (7) Cho, H.; Jeong, S. H.; Park, M. H.; Kim, Y. H.; Wolf, C.; Lee, C. L.; Heo, J. H.; Sadhanala, A.; Myoung, N.; Yoo, S.; Im, S. H.; Friend, R. H.; Lee, T. W. Overcoming The Electroluminescence Efficiency Limitations Of Perovskite Light-Emitting Diodes. *Science* 2015, 350, 1222.

- (8) Lin, K.; Xing, J.; Quan, L. N.; de Arquer, F. P. G.; Gong, X.; Lu, J.; Xie, L.; Zhao, W.; Zhang, D.; Yan, C.; Li, W.; Liu, X.; Lu, Y.; Kirman, J.; Sargent, E. H.; Xiong, Q.; Wei, Z. Perovskite light-emitting diodes with external quantum efficiency exceeding 20 per cent. *Nature* 2018, 562 (7726), 245-248.
- (9) Chiba, T.; Hayashi, Y.; Ebe, H.; Hoshi, K.; Sato, J.; Sato, S.; Pu, Y.-J.; Ohisa, S.; Kido, J. Anion-exchange red perovskite quantum dots with ammonium iodine salts for highly efficient light-emitting devices. *Nature Photonics* 2018, 12 (11), 681-687.
- (10) Xu, W.; Hu, Q.; Bai, S.; Bao, C.; Miao, Y.; Yuan, Z.; Borzda, T.; Barker, A. J.; Tyukalova, E.; Hu, Z.; Kawecki, M.; Wang, H.; Yan, Z.; Liu, X.; Shi, X.; Uvdal, K.; Fahlman, M.; Zhang, W.; Duchamp, M.; Liu, J.-M.; Petrozza, A.; Wang, J.; Liu, L.-M.; Huang, W.; Gao, F. Rational molecular passivation for high-performance perovskite light-emitting diodes. *Nature Photonics* 2019, 13 (6), 418-424.
- (11) Wang, Q.; Wang, X.; Yang, Z.; Zhou, N.; Deng, Y.; Zhao, J.; Xiao, X.; Rudd, P.; Moran, A.; Yan, Y.; Huang, J. Efficient sky-blue perovskite light-emitting diodes via photoluminescence enhancement. *Nature Communications* 2019, 10 (1), 5633.
- (12) Jung, M.-H.; Rhim, S. H.; Moon, D. TiO₂/RbPbI₃ halide perovskite solar cells. *Solar Energy Materials and Solar Cells* 2017, 172, 44-54.

- (13) Mitzi, D. B. Templating and structural engineering in organic–inorganic perovskites. *Journal of the Chemical Society, Dalton Transactions* 2001, (1), 1-12.
- (14) Liang, L.; Wencong, L.; Nianyi, C. On the criteria of formation and lattice distortion of perovskite-type complex halides. *Journal of Physics and Chemistry of Solids* 2004, 65 (5), 855-860.
- (15) Lee, B. R. A Study on Charge Selective Transport for Highly Efficient Polymer Based Optoelectronic Devices. Graduate school of UNIST.
- (16) D'Andrade, B. W.; Forrest, S. R. White Organic Light-Emitting Devices for Solid-State Lighting. *Adv. Mater.* 2004, 16, 1585.
- (17) Friend, R. H.; Gymer, R. W.; Holmes, A. B.; Burroughes, J. H.; Marks, R. N.; Taliani, C.; Bradley, D. D. C.; Dos Santos, D. A.; Bredas, J. L.; Logdlund, M. Electroluminescence in Conjugated Polymers. *Nature* 1999, 397, 121.
- (18) Gustafsson, G.; Cao, Y.; Treacy, G. M.; Klavetter, F.; Colaneri, N.; Heeger, A. J. Flexible Light-Emitting Diodes Made from Soluble Conducting Polymers. *Nature* 1992, 357, 477.
- (19) Ou, E. C. W.; Hu, L. B.; Raymond, G. C. R.; Soo, O. K.; Pan, J. S.; Zheng, Z.; Park, Y.; Hecht, D.; Irvin, G.; Drzaic, P. Surface-Modified Nanotube Anodes for High Performance Organic Light-Emitting Diode. *ACS Nano* 2009, 3, 2258.
- (20) Zhao, B.; Bai, S.; Kim, V.; Lamboll, R.; Shivanna, R.; Auras, F.; Richter, J. M.; Yang, L.; Dai, L.; Alsari, M.; She, X.-J.; Liang, L.; Zhang, J.; Lilliu, S.; Gao,

P.; Snaith, H. J.; Wang, J.; Greenham, N. C.; Friend, R. H.; Di, D. High-efficiency perovskite–polymer bulk heterostructure light-emitting diodes. *Nature Photonics* 2018, 12 (12), 783-789.

(21) Park, M.-H.; Park, J.; Lee, J.; So, H. S.; Kim, H.; Jeong, S.-H.; Han, T.-H.; Wolf, C.; Lee, H.; Yoo, S.; Lee, T.-W. Efficient Perovskite Light-Emitting Diodes Using Polycrystalline Core–Shell-Mimicked Nanograins. *Advanced Functional Materials* 2019, 29 (22), 1902017.

(22) Matsuoka, K.; Albrecht, K.; Nakayama, A.; Yamamoto, K.; Fujita, K. Highly Efficient Thermally Activated Delayed Fluorescence Organic Light-Emitting Diodes with Fully Solution-Processed Organic Multilayered Architecture: Impact of Terminal Substitution on Carbazole–Benzophenone Dendrimer and Interfacial Engineering. *ACS Applied Materials & Interfaces* 2018, 10 (39), 33343-33352.

(23) Liu, Q.-W.; Yuan, S.; Sun, S.-Q.; Luo, W.; Zhang, Y.-J.; Liao, L.-S.; Fung, M.-K. Interfacial engineering for highly efficient quasi-two dimensional organic–inorganic hybrid perovskite light-emitting diodes. *Journal of Materials Chemistry C* 2019, 7 (15), 4344-4349.

(24) Xing, J.; Yan, F.; Zhao, Y.; Chen, S.; Yu, H.; Zhang, Q.; Zeng, R.; Demir, H. V.; Sun, X.; Huan, A.; Xiong, Q. High-Efficiency Light-Emitting Diodes of Organometal Halide Perovskite Amorphous Nanoparticles. *ACS Nano* 2016, 10 (7), 6623-6630.

- (25) Ling, Y.; Yuan, Z.; Tian, Y.; Wang, X.; Wang, J. C.; Xin, Y.; Hanson, K.; Ma, B.; Gao, H. Bright Light-Emitting Diodes Based on Organometal Halide Perovskite Nanoplatelets. *Advanced Materials* 2016, 28 (2), 305-311.
- (26) Zhang, X.; Wang, W.; Xu, B.; Liu, S.; Dai, H.; Bian, D.; Chen, S.; Wang, K.; Sun, X. W. Thin film perovskite light-emitting diode based on CsPbBr₃ powders and interfacial engineering. *Nano Energy* 2017, 37, 40-45.
- (27) Tsuji, H.; Mitsui, C.; Sato, Y.; Nakamura, E. Bis(carbazolyl)benzodifuran: A High-Mobility Ambipolar Material for Homojunction Organic Light-Emitting Diode Devices. *Advanced Materials* 2009, 21 (37), 3776-3779.
- (28) Khotina, I. A.; Lepnev, L. S.; Burenkova, N. S.; Valetsky, P. M.; Vitukhnovsky, A. G. Phenylene dendrimers and novel hyperbranched polyphenylenes as light emissive materials for blue OLEDs. *Journal of Luminescence* 2004, 110 (4), 232-238.
- (29) Huang, H.; Zhao, F.; Liu, L.; Zhang, F.; Wu, X.-g.; Shi, L.; Zou, B.; Pei, Q.; Zhong, H. Emulsion Synthesis of Size-Tunable CH₃NH₃PbBr₃ Quantum Dots: An Alternative Route toward Efficient Light-Emitting Diodes. *ACS Applied Materials & Interfaces* 2015, 7 (51), 28128-28133.
- (30) Zhang, J.; Yang, Y.; Deng, H.; Farooq, U.; Yang, X.; Khan, J.; Tang, J.; Song, H. High Quantum Yield Blue Emission from Lead-Free Inorganic Antimony Halide Perovskite Colloidal Quantum Dots. *ACS Nano* 2017, 11 (9), 9294-9302.

- (31) Islam, A.; Wang, Q.; Zhang, L.; Lei, T.; Hong, L.; Yang, R.; Liu, Z.; Peng, R.; Liao, L.-S.; Ge, Z. Efficient non-doped deep blue organic light emitting diodes with high external quantum efficiency and a low efficiency roll-off based on donor-acceptor molecules. *Dyes and Pigments* 2017, 142, 499-506.
- (32) Wang, F.; Sun, W.; Liu, P.; Wang, Z.; Zhang, J.; Wei, J.; Li, Y.; Hayat, T.; Alsaedi, A.; Tan, Z. Achieving Balanced Charge Injection of Blue Quantum Dot Light-Emitting Diodes through Transport Layer Doping Strategies. *J Phys Chem Lett* 2019, 10 (5), 960-965.
- (33) Ohshita, J.; Tada, Y.; Kunai, A.; Harima, Y.; Kunugi, Y. Hole-injection properties of annealed polythiophene films to replace PEDOT-PSS in multilayered OLED systems. *Synthetic Metals* 2009, 159 (3), 214-217.
- (34) Lee, J. J.; Lee, S. H.; Kim, F. S.; Choi, H. H.; Kim, J. H. Simultaneous enhancement of the efficiency and stability of organic solar cells using PEDOT:PSS grafted with a PEGME buffer layer. *Organic Electronics* 2015, 26, 191-199.
- (35) Yun, J.-M.; Yeo, J.-S.; Kim, J.; Jeong, H.-G.; Kim, D.-Y.; Noh, Y.-J.; Kim, S.-S.; Ku, B.-C.; Na, S.-I. Solution-Processable Reduced Graphene Oxide as a Novel Alternative to PEDOT:PSS Hole Transport Layers for Highly Efficient and Stable Polymer Solar Cells. *Advanced Materials* 2011, 23 (42), 4923-4928.

- (36) Wang, Q.; Dong, Q.; Li, T.; Gruverman, A.; Huang, J. Thin Insulating Tunneling Contacts for Efficient and Water-Resistant Perovskite Solar Cells. *Advanced Materials* 2016, 28 (31), 6734-6739.
- (37) Ma, S.; Qiao, W.; Cheng, T.; Zhang, B.; Yao, J.; Alsaedi, A.; Hayat, T.; Ding, Y.; Tan, Z.; Dai, S. Optical-Electrical-Chemical Engineering of PEDOT:PSS by Incorporation of Hydrophobic Nafion for Efficient and Stable Perovskite Solar Cells. *ACS Appl Mater Interfaces* 2018, 10 (4), 3902-3911.
- (38) Kim, J. H.; Liang, P. W.; Williams, S. T.; Cho, N.; Chueh, C. C.; Glaz, M. S.; Ginger, D. S.; Jen, A. K. High-performance and environmentally stable planar heterojunction perovskite solar cells based on a solution-processed copper-doped nickel oxide hole-transporting layer. *Adv Mater* 2015, 27 (4), 695-701.
- (39) Meng, Y.; Wu, X.; Xiong, Z.; Lin, C.; Xiong, Z.; Blount, E.; Chen, P. Electrode quenching control for highly efficient CsPbBr₃ perovskite light-emitting diodes via surface plasmon resonance and enhanced hole injection by Au nanoparticles. *Nanotechnology* 2018, 29 (17), 175203.
- (40) Lin, C.; Chen, P.; Xiong, Z.; Liu, D.; Wang, G.; Meng, Y.; Song, Q. Interfacial engineering with ultrathin poly (9,9-di-n-octylfluorenyl-2,7-diyl) (PFO) layer for high efficient perovskite light-emitting diodes. *Nanotechnology* 2018, 29 (7), 075203.

- (41) Chen, W.; Wu, Y.; Yue, Y.; Liu, J.; Zhang, W.; Yang, X.; Chen, H.; Bi, E.; Ashraful, I.; Grätzel, M.; Han, L. Efficient and stable large-area perovskite solar cells with inorganic charge extraction layers. *Science* 2015, 350 (6263), 944-948.
- (42) Wang, Z.; Luo, Z.; Zhao, C.; Guo, Q.; Wang, Y.; Wang, F.; Bian, X.; Alsaedi, A.; Hayat, T.; Tan, Z. a. Efficient and Stable Pure Green All-Inorganic Perovskite CsPbBr₃ Light-Emitting Diodes with a Solution-Processed NiO_x Interlayer. *The Journal of Physical Chemistry C* 2017, 121 (50), 28132-28138.
- (43) Yang, X.; Ma, Y.; Mutlugun, E.; Zhao, Y.; Leck, K. S.; Tan, S. T.; Demir, H. V.; Zhang, Q.; Du, H.; Sun, X. W. Stable, Efficient, and All-Solution-Processed Quantum Dot Light-Emitting Diodes with Double-Sided Metal Oxide Nanoparticle Charge Transport Layers. *ACS Applied Materials & Interfaces* 2013, 6 (1), 495-499.
- (44) Li, Z. Stable Perovskite Solar Cells Based on WO₃ Nanocrystals as Hole Transport Layer. *Chemistry Letters* 2015, 44 (8), 1140-1141.
- (45) Elumalai, N. K.; Saha, A.; Vijila, C.; Jose, R.; Jie, Z.; Ramakrishna, S. Enhancing the stability of polymer solar cells by improving the conductivity of the nanostructured MoO₃ hole-transport layer. *Physical Chemistry Chemical Physics* 2013, 15 (18), 6831-6841.
- (46) Hu, X.; Chen, L.; Chen, Y. Universal and Versatile MoO₃-Based Hole Transport Layers for Efficient and Stable Polymer Solar Cells. *The Journal of Physical Chemistry C* 2014, 118 (19), 9930-9938.

- (47) Aboulsaad, M.; El Tahan, A.; Soliman, M.; El-Sheikh, S.; Ebrahim, S. Thermal oxidation of sputtered nickel nano-film as hole transport layer for high performance perovskite solar cells. *Journal of Materials Science: Materials in Electronics* 2019, 30 (22), 19792-19803.
- (48) Lee, S.; Kim, D. B.; Hamilton, I.; Daboczi, M.; Nam, Y. S.; Lee, B. R.; Zhao, B.; Jang, C. H.; Friend, R. H.; Kim, J.-S.; Song, M. H. Control of Interface Defects for Efficient and Stable Quasi-2D Perovskite Light-Emitting Diodes Using Nickel Oxide Hole Injection Layer. *Advanced Science* 2018, 5 (11), 1801350.
- (49) Kim, B.-S.; Kim, T.-M.; Choi, M.-S.; Shim, H.-S.; Kim, J.-J. Fully vacuum-processed perovskite solar cells with high open circuit voltage using MoO₃/NPB as hole extraction layers. *Organic Electronics* 2015, 17, 102-106.
- (50) Kyaw, A. K. K.; Sun, X. W.; Jiang, C. Y.; Lo, G. Q.; Zhao, D. W.; Kwong, D. L. An inverted organic solar cell employing a sol-gel derived ZnO electron selective layer and thermal evaporated MoO₃ hole selective layer. *Applied Physics Letters* 2008, 93 (22), 221107.
- (51) Shi, W.; Fan, S.; Huang, F.; Yang, W.; Liu, R.; Cao, Y. Synthesis of novel triphenylamine-based conjugated polyelectrolytes and their application as hole-transport layers in polymeric light-emitting diodes. *Journal of Materials Chemistry* 2006, 16 (24), 2387-2394.

- (52) Lee, S.; Jang, C. H.; Nguyen, T. L.; Kim, S. H.; Lee, K. M.; Chang, K.; Choi, S. S.; Kwak, S. K.; Woo, H. Y.; Song, M. H. Conjugated Polyelectrolytes as Multifunctional Passivating and Hole-Transporting Layers for Efficient Perovskite Light-Emitting Diodes. *Advanced Materials* 2019, 31 (24), 1900067.
- (53) Lee, B. R.; Yu, J. C.; Park, J. H.; Lee, S.; Mai, C. K.; Zhao, B.; Wong, M. S.; Jung, E. D.; Nam, Y. S.; Park, S. Y.; Di Nuzzo, D.; Kim, J. Y.; Stranks, S. D.; Bazan, G. C.; Choi, H.; Song, M. H.; Friend, R. H. Conjugated Polyelectrolytes as Efficient Hole Transport Layers in Perovskite Light-Emitting Diodes. *ACS Nano* 2018, 12 (6), 5826-5833.
- (54) Lee, B. R.; Kim, J.-w.; Kang, D.; Lee, D. W.; Ko, S.-J.; Lee, H. J.; Lee, C.-L.; Kim, J. Y.; Shin, H. S.; Song, M. H. Highly Efficient Polymer Light-Emitting Diodes Using Graphene Oxide as a Hole Transport Layer. *ACS Nano* 2012, 6 (4), 2984-2991.
- (55) Shi, S.; Sadhu, V.; Moubah, R.; Schmerber, G.; Bao, Q.; Silva, S. R. P. Solution-processable graphene oxide as an efficient hole injection layer for high luminance organic light-emitting diodes. *Journal of Materials Chemistry C* 2013, 1 (9), 1708-1712.
- (56) Diker, H.; Bozkurt, H.; Varlikli, C. Dispersion stability of amine modified graphene oxides and their utilization in solution processed blue OLED. *Chemical Engineering Journal* 2020, 381, 122716.

(57) Kim, T. G.; Ha, S. R.; Choi, H.; Uh, K.; Kundapur, U.; Park, S.; Lee, C. W.; Lee, S. H.; Kim, J.; Kim, J. M. Polymerizable Supramolecular Approach to Highly Conductive PEDOT:PSS Patterns. *ACS Appl Mater Interfaces* 2017, 9 (22), 19231-19237.

(58) Ha, S. R.; Park, S.; Oh, J. T.; Kim, D. H.; Cho, S.; Bae, S. Y.; Kang, D.-W.; Kim, J.-M.; Choi, H. Water-resistant PEDOT:PSS hole transport layers by incorporating a photo-crosslinking agent for high-performance perovskite and polymer solar cells. *Nanoscale* 2018, 10 (27), 13187-13193.

(59) Li, W.; Zhang, X.; Zhang, X.; Yao, J.; Zhan, C. High-Performance Solution-Processed Single-Junction Polymer Solar Cell Achievable by Post-Treatment of PEDOT:PSS Layer with Water-Containing Methanol. *ACS Applied Materials & Interfaces* 2017, 9 (2), 1446-1452.

(60) Chen, K.; Hu, Q.; Liu, T.; Zhao, L.; Luo, D.; Wu, J.; Zhang, Y.; Zhang, W.; Liu, F.; Russell, T. P.; Zhu, R.; Gong, Q. Charge-Carrier Balance for Highly Efficient Inverted Planar Heterojunction Perovskite Solar Cells. *Advanced Materials* 2016, 28 (48), 10718-10724.

Acknowledgement

How time flies, it means my master's career is coming to an end when I write here. I still remember the tense and unconfident feeling when I entered Pukyong National University for the first time, but actually, I am not under too much pressure, I have been studying and researching in a relaxed environment, because I have good teachers and friends.

First of all, I sincerely appreciate my advisor, Professor Bo Ram Lee, this thesis was completed under his careful guidance. During the two years' master degree course, he gave me a lot of support and encouragement in my study and life. In my impression, the most words he said to me is "Don't worry", here I express my heartfelt gratitude to him.

Secondly, I am much obliged to Professor Jung Hyun Jeong and Professor Ruijin Yu. It was they who gave me the opportunity to study in Pukyong National University, this experience will be a key point in my future life. In addition, I would like to extend my sincere gratitude to Professor Sung Heum Park, I took his class every semester, he taught me a lot of knowledge of our major.

Thirdly, I am very truly grateful to all HOME and ODPL members, they helped me solve inconveniences in life and problems in research. At the same time, thank all my Chinese friends for their companionship.

Lastly, I deeply appreciate my family for their support and care, I will work harder in my future life and live up to their expectations.